JOURNAL OF GEOPHYSICAL RESEARCH, VOL. 102, NO. D15, PAGES 19,207–19,216, AUGUST 20, 1997

Temperature dependence of the ClO concentration near the stratopause

S. Ghosh[1], J.A. Pyle, and P. Good

Centre for Atmospheric Science, Department of Chemistry, University of Cambridge, Cambridge England

Abstract. From an analysis of Microwave Limb Sounder (MLS) ClO data near the stratopause where it is reasonable to assume that ClO is in photochemical equilibrium, it is found that there is a strong temperature dependence of the order of 1000 K(±200 K) including the effects of scaling and the bias uncertainties in the retrieved MLS data. Results from a three- dimensional model (extended UK Universities Global Atmospheric Modelling Programme (UGAMP) general circulation model (EUGCM)) agree well with the MLS results; we obtain a temperature dependence of 950 K in the three-dimensional model. The temperature dependencies obtained from the MLS data and the EUGCM agree quite well with results from a purely photochemical box model which yields a temperature dependence of the order of 900 K. The generally good agreement between the temperature dependence of ClO obtained from the MLS measurements, from both the photochemical model and the three- dimensional general circulation model does not suggest that there are major uncertainties in our understanding of the ClO chemistry in the upper stratosphere.

1. Introduction

Chlorine compounds play a vital part in stratospheric chemistry. Their role in ozone depletion in the lower stratosphere is well documented[see, e.g., *World Meteorological Organisation*, 1994]. Chlorine compounds can also destroy ozone in catalytic cycles in the upper stratosphere. Indeed, in the paper which originally alerted the scientific community to the threat to stratospheric ozone posed by the buildup of chlorofluorocarbons [*Molina and Rowland*, 1974], it was predicted that ozone loss would occur predominantly in the upper stratosphere. That expectation remained until the discovery of the "ozone hole" [*Farman et al.*, 1985] and much subsequent work has reported the special role of heterogeneous chemistry in the lower stratosphere, the key to understanding polar ozone depletion.

Given that chlorine compounds are so important to stratospheric chemistry, it is important that their atmospheric chemistry is well understood. Without this detailed understanding, predictions about future change cannot be made with confidence. One way of confirming understanding is by comparing observations with numerical model predictions. This is very important, but in complex systems with many variables it is often difficult to configure the model to represent the atmosphere accurately. An alternative method is to isolate some closed subset of the system. Thus, in the upper stratosphere where ozone is close to photochemical equilibrium, the variation of ozone concentration with temperature provides an excellent test of photochemical theory [*Barnett et al.*, 1975; *Froidevaux et al.*, 1989].

In this study, we have attempted to test our understanding of gas phase chlorine chemistry using a combination of satellite data and numerical models. A very important and novel data set for global ClO has been provided by the Microwave limb sounder (MLS) experiment on the Upper Atmosphere Research Satellite (UARS). One of the most spectacular successes of the MLS data has been to show the global structure in ClO in the lower stratosphere. During the winter and spring in both hemispheres, *Waters et al.*, [1993] and *Manney et al.*, [1994] have shown examples when each polar vortex is filled with elevated ClO. High ClO in the northern hemisphere has been shown to be consistent with ozone loss also measured by MLS [*Waters et al.*, 1993]. In this paper we have used the MLS data to calculate the temperature dependence of ClO in the upper stratosphere. These results are compared with theory, using both a simple box model and a three-dimensional general circulation model including a detailed description of stratospheric chemistry.

The next section briefly summarizes the chemistry of chlorine in the upper stratosphere. Then we describe the MLS data, including a description of the observational errors, and the calculation of the ClO temperature dependence. Finally, we use models to determine the temperature dependence expected theoretically.

[1]Now at Department of Physics, University of Manchester Institute of Science and Technology, Manchester, England.

Paper number 97JD01099.
0148-0227/97/97JD-01099$09.00

2. ClO Chemistry

The most important fate of the chlorine atoms released in the stratosphere by the photodecomposition of chlorofluorocarbons is reaction with ozone to form ClO:

$$Cl + O_3 \rightarrow ClO + O_2 \qquad (k_2) \qquad (1)$$

Chlorine monoxide reacts with atomic oxygen to regenerate the chlorine atom, thereby completing a catalytic cycle which destroys ozone:

$$ClO + O \rightarrow Cl + O_2 \qquad (k_3) \qquad (2)$$

It can also react with NO:

$$ClO + NO \rightarrow Cl + NO_2 \qquad (k_4) \qquad (3)$$

In addition to these rapid processes which largely determine an equilibrium between Cl and ClO, there are also slower proceses which cycle Cl and ClO into, and from, HCl, $ClONO_2$, and HOCl (see Table 1).

Photochemical equilibrium can only be assumed if the species in question interchange with one another considerably more rapidly than they can be influenced by transport. This should certainly be true for ClO near the stratopause (where the photochemical lifetime is of the order of seconds). We can then evaluate the equilibrium ratio between chlorine- containing compounds to serve as a rough estimate of their relative abundances.

From the ClO chemistry just discussed, and with the assumption of photochemical equilibrium, one can in principle obtain the partitioning between the various species. For ClO and Cl, this can be expressed as

$$\frac{[ClO]}{[Cl]} \simeq \frac{k_2[O_3]}{(k_3[O] + k_4[NO])} \qquad (4)$$

Assuming photochemical equilibrium for ClO and HOCl and retaining only the most important terms [*Brasseur and Solomon*, 1986] we have

$$\frac{[ClO]}{[HOCl]} \simeq \frac{J_{HOCl} + k_{34}[OH]}{k_{33}[HO_2]} \qquad (5)$$

Similar arguments can also be applied for $ClONO_2$, HCl and ClO and one may obtain

$$\frac{[ClO]}{[ClONO_2]} \simeq \frac{J_{ClONO_2} + k_{32}[O]}{k_{31}[M][NO_2]} \qquad (6)$$

$$\frac{[ClO]}{[HCl]} \simeq \frac{k_2[O_3]k_{11}[OH]}{(k_3[O] + k_4[NO])(k_5[CH_4] + k_7[HO_2] + k_{10}[CH_2O])} \qquad (7)$$

The equilibrium expressions (4), (5), (6) and (7) are all temperature dependent. Many of the rate constants involved have a temperature dependence. In addition, the concentrations of the various species involved in the equilibrium expression will themselves vary with temperature, through their dependence on other temperature dependent reactions. (For example, the ozone concentration has been shown to be strongly temperature dependent around the stratopause [*Barnett et al.*, 1975; *Froidevaux et al.*, 1989]).

From these equations, the temperature dependence of ClO can be calculated, either analytically or using a numerical model. The ClO concentration in the lower stratosphere depends in a complex way on temperature and gas phase and heterogeneous chemistry. Reactions on sulphate aerosol particles as well as on polar stratospheric clouds are important. Determination of the temperature dependence is more complex than chemistry in the upper stratosphere where gas phase chemistry plays the dominant role. For this reason, this study concentrates on the upper stratosphere. The important chlorine species (Cl, ClO, HCl, HOCl) are to a very good approximation in photochemical equilibrium there, as discussed above. Thus studies in the region should be a good test of photochemical understanding. Here we will use two different models to cal-

Table 1. Some Reactions Involving Cl and ClO Chemistry in Mid-Upper Stratosphere

Reaction	Rate Constant Name	A, $cm^3mol^{-1}s^{-1}$	E/R ± (ΔE/R)	k(298)	f(298)
$Cl + O_3 \rightarrow ClO + O_2$	(k_2)	2.9×10^{-11}	260 ± 100	1.2×10^{-11}	1.15
$ClO + O \rightarrow Cl + O_2$	(k_3)	3.0×10^{-11}	-(70± 70)	3.8×10^{-11}	1.2
$ClO + NO \rightarrow Cl + NO_2$	(k_4)	6.4×10^{-12}	-(290±100)	1.7×10^{-11}	1.15
$Cl + CH_4 \rightarrow CH_3 + HCl$	(k_5)	1.1×10^{-11}	(1400± 150)	1.0×10^{-13}	1.1
$Cl + HO_2 \rightarrow O_2 + HCl$	(k_7)	1.8×10^{-11}	-(170± 200)	3.2×10^{-11}	1.5
$Cl + CH_2O \rightarrow HCO + HCl$	(k_{10})	8.1×10^{-11}	(30± 100)	7.3×10^{-11}	1.15
$HCl + OH \rightarrow H_2O + Cl$	(k_{11})	2.6×10^{-12}	(350± 100)	8.0×10^{-13}	1.3
$HCl + O \rightarrow OH + Cl$	(k_{12})	1.0×10^{-11}	(3300± 350)	1.5×10^{-16}	2.0
$ClO + NO_2 + M \rightarrow ClONO_2 + M$	(k_{31})	(see text)			
$ClONO_2 + O \rightarrow$ products	(k_{32})	2.9×10^{-12}	(800± 200)	2.0×10^{-13}	1.5
$HO_2 + ClO \rightarrow HOCl + O_2$	(k_{33})	4.8×10^{-13}	(100± 250)	5.0×10^{-12}	1.4
$OH + HOCl \rightarrow H_2O + ClO$	(k_{34})	3.0×10^{-12}	(500±500)	5.0×10^{-13}	3.0
$ClONO_2 + h\nu \rightarrow Cl + NO_3$	(J_{ClONO_2})				
$HOCl + h\nu(\lambda < 301nm) \rightarrow ClO + H$	(J_{HOCl})				
$HOCl + h\nu(\lambda < 503nm) \rightarrow Cl + OH$	(J_{HOCl})				

culate the temperature dependence. First, in the next section, we consider the temperature dependence found in the stratosphere using MLS data. Then we compare the observed temperature dependence with that derived from a three-dimensional transport model including a detailed chemical scheme. Comparison will serve as a test of the chemistry outlined above.

We have chosen to use a full three-dimensional model for this study because even under conditions of photochemical equilibrium, there is obviously some dependence on the atmospheric circulation (for example, this determines the overall concentrations of source gases). We have chosen here not to perform an analytical study (as done by *Barnett et al.* [1975] and *Froidevaux et al.* [1989] for ozone) which would isolate chemical dependencies but ignore any circulation effects. We believe our approach is most appropriate when comparing stratospheric data, which will depend on chemical and dynamical conditions, with theory. However, we have explicitly tested the sensitivity of our results to the chemical scheme used by performing some box model calculations, presented later.

3. Observations

3.1. Overview

The Microwave Limb Sounder (MLS) was launched on September 12, 1991, on the Upper Atmosphere Research Satellite (UARS). MLS is the first satelliteborne instrument for constituent limb sounding using the microwave region of the spectrum. The instrument has three radiometers simultaneously measuring millimeter-wavelength thermal emission in spectral bands near 205 GHz (for ClO and O_3) [see, e.g., *Waters et al.*, 1993], 63 GHz (temperature and pressure) and 183 GHz (for H_2O and O_3) [see, e.g., *Froidevaux et al.*, 1994]. Measurement coverage is from 80°N on one side of the equator to 34° on the other. There are 15 orbits per day, and the orbit plane precesses slowly with respect to the Sun-Earth direction, so that the local solar time of MLS measurements at a given latitude (on either the "day" or "night" side of the orbit) varies by 20 min during a 24- hour period. UARS performs a "yaw manoevre" when the orbit precesses through 180° (10 times per year), so MLS high latitude coverage switches between north and south every 36 days. Measurements are made continuously day and night and are not degraded by stratospheric clouds or aerosols.

3.2. Error Analysis

The preceding section briefly described the MLS data. In this section, we describe the expected errors in the retrievals reported by the MLS team.

It should be emphasized that the UARS MLS design was "frozen" before the discovery of the severe ozone loss in the lower stratosphere over Antarctica, at a time when the major concerns were chlorine depletion of ozone in the upper stratosphere. Consequently, the instrument is principally designed for measurements in the middle and the upper stratosphere.

From the current documentation available [e.g., *Waters et al.*,1996] on the use of MLS data, we know that the version 3 data are principally useful for scientific analyses at retrieval surfaces between 46 and 1 hPa (approximately 20 to 50 km height) [*Waters et al.*, 1996]. In this study, we have examined MLS ClO and temperature data at 1.5 hPa, within the permissible analysis region. A detailed account of the the various types of uncertainties originating in the MLS data is given by *Waters et al.*, [1996]. In this section we will only briefly describe the various uncertainties which are incorporated into our analysis.

The uncertainties in the data are principally of three kinds [*Waters et al.*, 1996]:

1. Noise is a random contribution. The estimated uncertainty associated with each retrieved ClO profile point is obtained from the appropriate diagonal element of the estimated covariance matrix computed by the retrieval algorithms and is stored with retrieved values in the MLS data files. The uncertainty includes the effects of noise uncertainties associated with temperature, pointing, water vapor, fitted spectral baseline, and other parameters which are part of the overall state vector for the MLS retrievals.

Since noise is a random contribution, it can be greatly reduced by averaging. In the present analysis we have averaged over more than 9000 data points, and hence we expect the noise uncertainty to be smoothed out (see later in this section).

2. Scaling is a "multiplicative" uncertainty in the measurements and is given as a percentage. There is an overall instrument calibration uncertainty (combining systematic uncertainty in the calibrated radiances from each intrument channel with that introduced by instrument parameters in the radiance calculation) of 3%. Uncertainties in the absolute value of the absorption coefficient are due to uncertainties in the measured dipole moment of ClO and in the calculated matrix element for the particular transition observed by MLS.

3. Bias is essentially an additive uncertainty and can be introduced in the retrievals due to lack of adequately fitting the measured radiances within the noise. This residual uncertainty can be caused by inadequacies in the non-iterative linear algorithm used for producing version 3 data, and effects of interfering species which are not adequately accounted for in the retrieval scheme. The bias uncertainty can sometimes be appreciably reduced by taking appropriate day and nighttime differences [*Dessler et al.*, 1996; *Waters et al.*, 1996].

In the present analyses, we accessed MLS level 3 data from the Geophysical Data Facility at the Rutherford Appleton Laboratory. Certain systematic effects are observed in the temperature field. Zonal mean differences and zonal RMS difference between the MLS temperature field and the National Meteorological Center (NMC) analysis show biases which depend on whether the data is obtained during the ascending or descending side of the UARS orbit, whether MLS is looking north or south, and when during a yaw period measurements are taken [*Fishbein et al.*, 1996]. The systematics are 1-3 K in the stratosphere but can be as much as 10 K

in the lower mesosphere. MLS temperatures are biased 1-2 K lower than NMC temperatures between 22 and 1 hPa. In the winter at high latitudes, the atmosphere may differ from the linearization point by more than 20 K, especially when wave activity is enhanced. During these periods, systematic errors from nonlinearities may be of the order of 5-10 K. Wave amplitudes may be misrepresented during periods of large wave activity.

Systematic effects are also observed in the ClO measurements. HNO_3 and N_2O affect the lower stratosphere ClO retrievals, and the algorithms producing the version 3 level 3A files assume climatological values for these species. This leads to systematic errors up to 0.5 parts per billion by volume (ppbv) in the polar vortices and up to approximately 0.2 ppbv in other situations. In Table 2, we summarize the expected uncertainties in the MLS ClO and temperature data near the stratopause.

It is believed that the systematic "bias" and "scaling" uncertainties given above represent envelopes which are not often exceeded and are within 90% confidence (2σ) values [*Waters et al.*, 1996]. The bias and the scaling errors are calculated once the noise has been removed.

3.3. Observed Temperature Dependence

We have chosen to use MLS data, to calculate the temperature dependence of ClO. The data must be chosen appropriate to this study. It is clear from the discussion above that we cannot use single profile data. The noise on an individual profile is too large, and its use is likely to lead to spurious results. Secondly, ClO concentration in the atmosphere will depend not just on temperature but other processes too. For example, large scale dynamical factors are likely to influence [ClO]. On short timescales, [ClO] will exhibit a diurnal variation which is independent of temperature.

To avoid the latter problem we have used a very limited set of zenith angles. We have selected only zenith angles away from sunrise and sunset for which we believe the diurnal variation should not be large. Also, we chose to look in midlatitudes of the winter hemisphere, this being the only region where there is a large variation of temperature for a relatively small change in zenith angle.

We note that an instrument working in the microwave region of the spectrum is particularly suited for studies of temperature dependence since, in the microwave, the retrieval of constituent concentrations is itself not strongly temperature dependent.

For this study, we have used the ClO measurements at 1.47 hPa between October 1991 to December 1991. In order to minimize the effect of random error in the ClO data, we have worked with averaged data. From Table 2, we find that for about 9000 data points the noise error associated with the ClO measurements is about 0.01 ppbv and for the temperature measurements is about 0.02 K at 1.5 hPa. These values are small and can be neglected. The bias and the scaling uncertainties are still important. Typically, at 0.5 ppbv ClO, the combined effect of both these uncertainties at the 1σ level is around 0.114 ppb; at 240 K the total effect of the temperature uncertainty is around 6 K.

To avoid problems associated with the diurnal variation of ClO, where concentrations should change rapidly, we have only used data at solar zenith angles (SZA) between 50^o and 70^o. All appropriate ClO and temperature data were extracted for the period October 1, 1991 to December 1, 1991. The data were then averaged and binned into 9 bins from 230 K to 275 K at intervals of 5 K. Whenever the temperature was between a prescribed range (for example, 230-235 K), all the ClO data, irrespective of position, were picked up and then averaged. This procedure was repeated for every temperature bin. Considering the fact that there were at least 600 data points in each bin, the noise error in the ClO data would be ~0.04 ppbv, and in the temperature data, it would be ~ 0.08K, which are again small.

We observe an anticorrelation between ClO and T. In Figure 1, we plot ln(ClO) against 1/T. The slope of the regression line gives a temperature dependence for the MLS data of 1009 K. There is an uncertainty in the slope estimate which we have investigated.

Several combinations of these errors were incorporated into each test case. The calculation of the temperature dependence was repeated, including in the calculation the errors in [ClO] or temperature discussed earlier. The overall shapes of the temperature dependence curves are essentially the same as in Figure 1 for the test cases and are therefore not shown explicitly. The main results are summarized in Table 3. In this table, we designate α and β as the scaling and bias uncertainties, respectively, at the 1 σ level for ClO. Likewise, γ and δ are the corresponding parameters for temperature. The last two columns in the table refer to the slope of the regression line (and hence the estimated temperature dependence) and the errors in the least squares fit for the slope estimation.

Several interesting observations can be made from Table 3. If one were to account for the scaling and the bias uncertainties in the ClO data alone, ignoring the temperature uncertainties, then one obtains a temperature dependence of ~1100 K with a negative bias

Table 2. Summary of MLS Errors Near the Stratopause

Pressure, hPa	Parameter	Single Profile 1σ Noise	Bias Uncertainty	Scaling Uncertainty, %
1.0	ClO	1.3 ppbv	0.2 ppbv	20.0
2.2	ClO	0.8 ppbv	0.15 ppbv	15.0
1.0	T	2.5 K	1-2 K	05.0
2.2	T	1.5 K	1-2 K	05.0

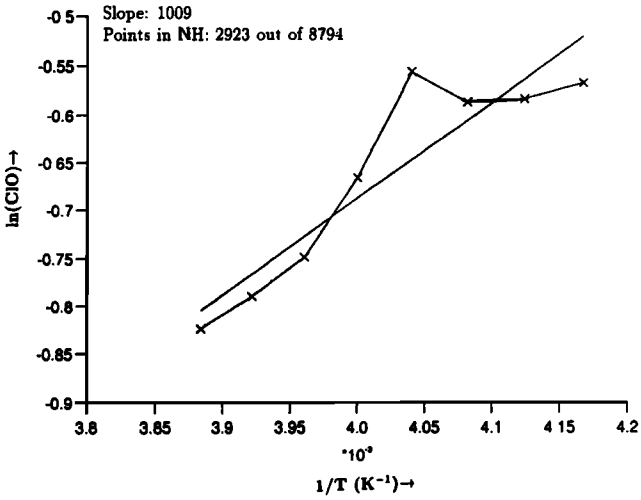

Figure 1. Temperature dependence of ClO calculated from Microwave Limb Sounder (MLS) observations.

uncertainty, irrespective of whether the scaling uncertainty is positive or negative. In contrast, one obtains a lower temperature dependence of ~900 K when the bias uncertainty is positive, and this is again independent of whether the scaling uncertainty is positive or negative. These results are not surprising given the nature of our analysis. A constant scaling will not change the difference in the ln[ClO], but a bias will play a role. If we were to consider the effect of only a positive temperture bias while ignoring the ClO errors, then we would obtain a temperature dependence of ~ 1000 K. Finally, when we include both the scaling and bias uncertainties in *both* ClO and T, we obtain a temperature dependence ~900 K. From the last column of Table 3 we find that the estimated error in the least squares fit to the slope of the ln(ClO) versus 1/T graph is generally of the order of ~20% for all the cases examined.

From the analysis presented in this section we have shown that by accounting for the scaling and the bias uncertainties in the retrieved MLS data and by allowing these uncertainties to propagate through the data set, the observed ClO temperature dependence is found to be of the order of 1000 K(±200 K).

4. Results From the 3-D Model

The temperature dependence derived from the MLS will depend on all the relevant atmospheric factors, both chemical and dynamical. It is therefore useful to compare this temperature dependence with the calculations in a three-dimensional model in which, it is hoped, the same factors are included. This is done in this section.

The UK Universities Global Atmospheric Modelling Programme (UGAMP) is a collaborative project involving a number of atmospheric science research institutes. One of the main aims is to study global scale dynamical, radiative, and chemical interactions in the middle atmosphere. In order to do this a 19 level forecast model provided by the European Centre for Medium-Range Weather Forecasting (ECMWF) (which reaches to approximately 30 km) has been extended to 47 levels (approximately 90 km) [*Gray et al.*, 1993]. The model consists of prognostic equations for vorticity, divergence, temperature, specific humidity, and surface pressure. In extending the ECMWF model, the lowest 16 levels of the original model have been left intact (i.e., up to 70 mbar), and smoothly varying vertical levels have been added above these, giving a vertical resolution throughout the stratosphere of 2-3 km. A hybrid vertical coordinate scheme is employed and vertical derivatives are calculated by taking finite differences. Spectral coefficients are used to represent the horizonatal variables. All model results presented here have been run at T21 horizontal resolution (approximately $6^o \times 6^o$). The equations are integrated in time using semi-implicit methods.

A sophisticated radiative scheme [*Morcrette*, 1990] and a gravity wave drag scheme [*Palmer et al.*, 1986] including the effects of both orographic as well as non-orographic gravity waves are also included in the model runs. The extended UGAMP general circulation model (EUGCM) was modified to include full interactive stratospheric chemistry between 326-0.1 mbar with all of the important species within the O_x, NO_x, ClO_x, and HO_x families. In this comprehensive photochemical package [*Lary et al.*, 1994] the rate constants were taken from *De More et al.*, [1994].

The initial chemical fields were taken from the Cambridge University two-dimensional model [*Chipperfield and Pyle*, 1990] except for NO_x and HNO_3 which were initialized with limb infrared monitor of the stratosphere (LIMS) data. The Cambridge two-dimensional model follows the classical Eulerian formulation; it calculates consistent temperatures from UV heating rates, with modeled ozone concentrations and the longwave radiation scheme of it Haigh [1984].

The initial meteorological conditions were from the ECMWF for October 28, 1991 with Stratospheric Sounding Unit (SSU) temperatures and geostrophic winds

Table 3. Test Cases for MLS Errors in ClO and T

α, %	β, ppbv	γ, K	δ, K	Slope, K	Error in Least Squares Fit, K
9.0	0.09	0.0	0.00	905.2	±165.4
9.0	-0.09	0.0	0.00	1124.3	±192.2
-9.0	0.09	0.0	0.00	887.4	±162.7
-9.0	-0.09	0.0	0.00	1147.9	±194.3
0.0	0.00	2.5	0.75	1004.6	±199.0
9.0	0.09	2.5	0.75	901.8	±185.2

above 30 mbar and an isothermal atmosphere with no vertical wind shear above 0.1 mbar. The model was then integrated forward in time for 70 days.

Figures 2 and 3 show the ClO and temperature respectively at 1.5 mbar for November 16 at local noon for solar zenith angles between 50° and 70°, as in the MLS retrievals. From these figures, it is observed that high values of ClO are found to be correlated with low temperatures. In Figures 4a and 4b, we show a plot of ln(ClO) against 1/T at 41.5°N and at 58.14°N from the model. We find a temperature dependence of 1011 K (at 41.5°N) and 950 K (58°N) in close agreement with those obtained from MLS data (Figure 1).

A plot of $dClO_x/dt$ for the same date is given in Figure 5. In the model, ClOx is defined as the sum of $(ClO+Cl+2Cl_2O_2)$. Since the Cl and Cl_2O_2 concentrations are very small at 1.5 mbar, $dClO_x/dt \simeq dClO/dt$. When this rate of change is zero, the ClO concentration is in photochemical equilibrium. From an examination of this figure, we find that close to a latitude circle of 58°N this condition holds. In Figure 6, we plot the temperature dependence of ClOx at 58°N, and we find that the temperature dependence is 938 K (very close to the value found for ClO). It is interesting to compare this with Figure 4a for the latitude circle at 41.5°N where the condition of photochemical equilibrium was not so strictly valid. We find a slightly different temperature dependence between the two graphs as expected.

As a final check on the accuracy of the EUGCM results, we also studied the temperature dependence of the ratio ClO_x/ClO_y (ClO_y being the total chlorine).

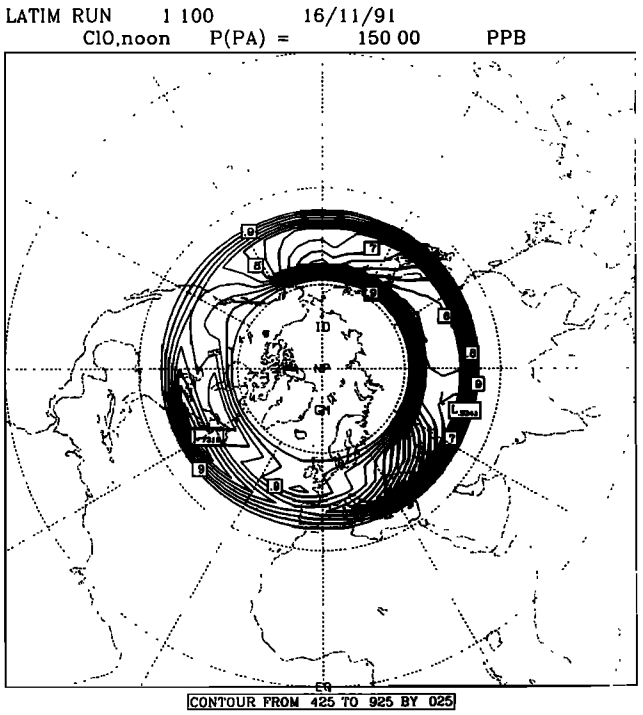

Figure 2. ClO (parts per billion by volume) from the extended UK Universities Global Atmospheric Modelling Program (EUGCM) for November 16, 1991, at 1.5 hPa. Calculated values are shown for zenith angles between 50° and 70°.

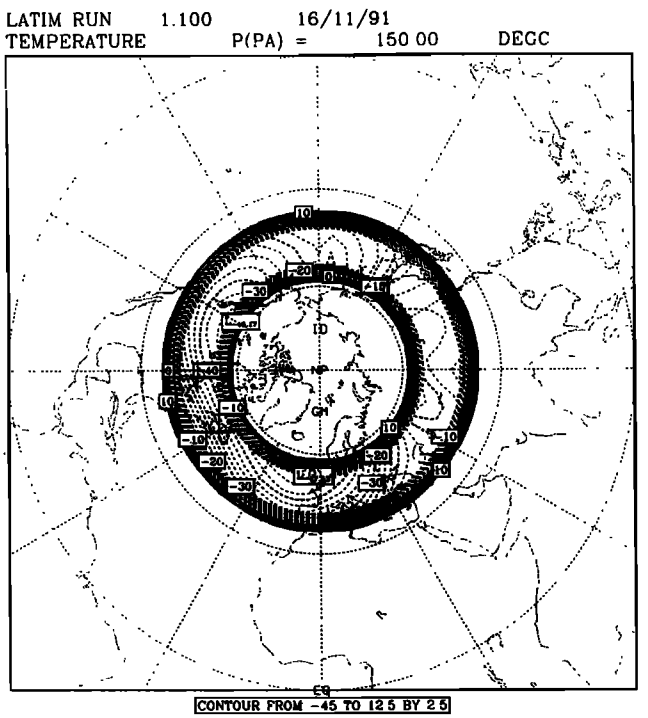

Figure 3. Temperature (Kelvins) from the EUGCM for November 16, 1991 at 1.5 hPa. Calculated values are shown for zenith angles between 50° and 70°.

Since the total chlorine in the model is conserved, the temperature dependence of the above ratio should be the same as that of ClO_x. We found that indeed the predicted temperature dependence of the above ratio is equal to that for ClO_x.

5. Error Discussion in the EUGCM

Ideally, it would be useful to perform a quantitative error analysis for the EUGCM results as was done for the MLS results in section 3. At this stage of our research, we are only able to give a qualitative discussion of the main sources of temperature errors likely to be associated with the EUGCM. First, we point to the fact that the present runs were performed at T21 horizontal resolution (appoximately 6° × 6°). That the horizontal resolution has a strong bearing on model performance was shown by *Mahlman and Umscheid* [1987]. They found that the strong polar night jet and the usually associated excessively cold polar temperatures that are encountered in general circulation models (GCMs) are drastically improved when the resolution is increased from 5° to 1°. In addition, these authors have analyzed the mean temperature profiles at 62°N for the 9°, 5°, 3°, and 1° resolution models. This study reveals a dramatic improvement of the polar cold bias as horizonatal resolution is increased. Such studies have not been performed to date with the EUGCM.

A second source of uncertainty is likely to be associated with the gravity wave drag parameterization. Although both orographic and nonorographic gravity waves are included in the present runs, there may be better schemes [e.g.,*Rind et al.*, 1988] where the gravity

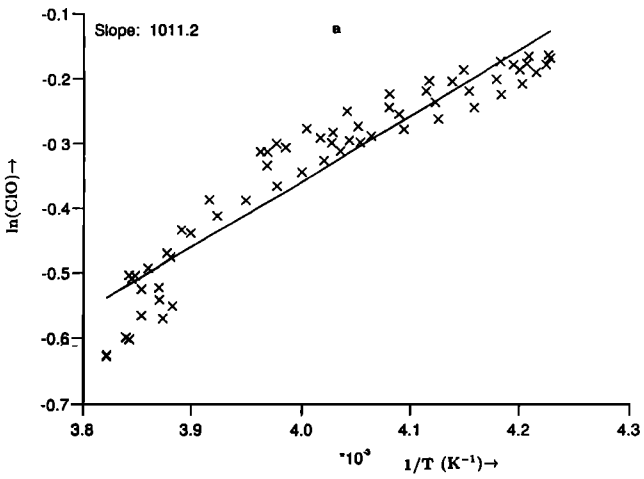

Figure 4a. Temperature dependence of ClO at 41.5°N and at 1.5 hPa calculated from the EUGCM.

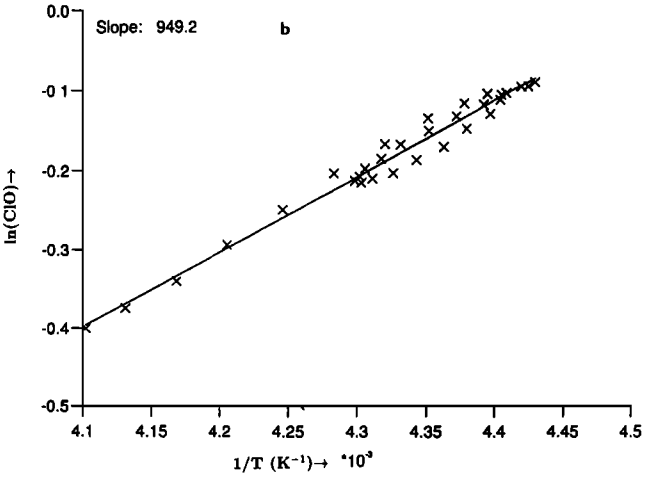

Figure 4b. Temperature dependence of ClO at 58°N and at 1.5 hPa calculated from the EUGCM.

wave phase velocities and momentum fluxes can be calculated in a more sophisticated manner than the scheme described by *Palmer et al.* [1986].

With regard to the radiation, a sophisticated radiation scheme [*Morcrette*, 1990] has been used. This scheme is known not to produce warm biases in the lower stratosphere, and hence the temperatures obtained from the present runs are expected to be free from extraneous biases. In fact, it was found that although the winter pole in the northern hemisphere is highly variable, the stratopause temperatures in the EUGCM are fairly accurate (J. Thuburn, private communication,1995). In this study, we are mainly concerned with temperatures around the stratopause and at latitudes closer to the surf zones than to the pole. We expect that model temperatures in the present analysis do not introduce a large error in our analysis. Note, also, that a model temperature error will not necessarily propagate as an error in the ClO temperature dependence. This is much more likely to arise from inaccuracies in the photochemical scheme (see below).

6. Photochemical Theory and Box Model Runs

The previous calculations give the overall temperature dependence due to both chemistry and dynamics. The difference between the calculations at different latitudes suggest that, while the photochemical contribution may be the major factor, dynamically driven temperature dependencies are also important. This justifies our decision to make the comparison with stratospheric data by using a 3-D chemistry and transport model. In this section, a purely photochemical model is used to isolate the chemical contribution.

We present results from a series of box model calculations run at different temperatures. The box model was initialized from concentrations obtained from the EUGCM and was then integrated at a fixed latitude and day of the year until the species attained photochemical equilibrium.

Figure 7 shows the temperature dependence of the ratio [ClO]/[HCl] from the box model run using equation (7). This gives a temperature dependence of 1306 K in good agreement with the value of 1398 K obtained from the corresponding EUGCM run (Figure 8).

Figure 9 shows the temperature dependence of the ratio [ClO]/[HOCl] from the box model run using equation (5). Again, this agrees well with the EUGCM result (Figure 10).

Finally, in Figure 11, we show the temperature dependence of ClO as obtained from the box model run to steady state. The box model output shown in Figure 11 corresponds to 58°N with varying solar zenith an-

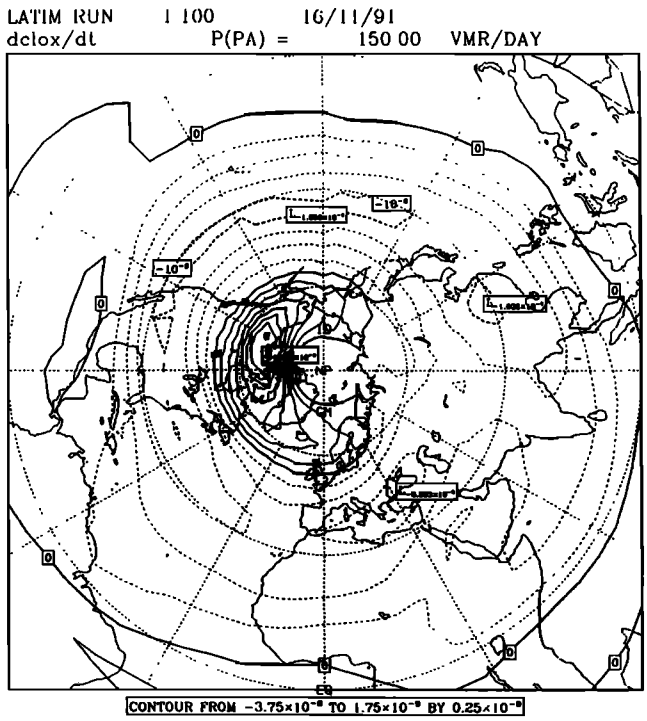

Figure 5. Rate of change of ClOx (dClOx/dt) in units of volume mixing ratio per day (vmr/day) from an EUGCM run November 16, 1991 at 1.5 hPa.

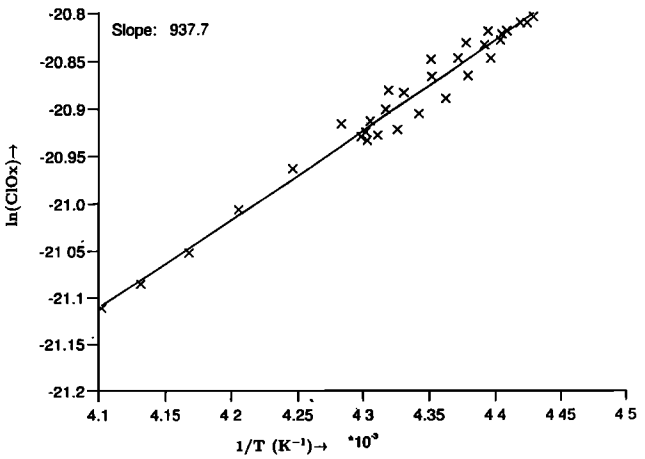

Figure 6. Temperature dependence of ClOx at 1.5 hPa and at 58°N calculated from the EUGCM.

gles throughout the day. This is therefore the temperature dependence one would expect from photochemical theory. We obtain a slope of 908 K which is in good agreement with the temperature dependences obtained from the EUGCM runs at 58°N. The slope is somewhat lower than but within the error bands of the temperature dependence from the MLS data.

7. Sensitivity Studies With the Photochemical Box Model

We have used the box model for two further sensitivity studies. In the first, we have performed an error analysis in which selected temperature dependent rate constants are varied within their expected errors. This study should indicate possible error bounds on our overall determination of the temperature dependence using the 3-D model and help indicate the reactions important in determining the temperature dependence. In the second sensitivity study, we have analyzed the dependence of the overall temperature dependence on three selected terms occurring in the photochemical scheme.

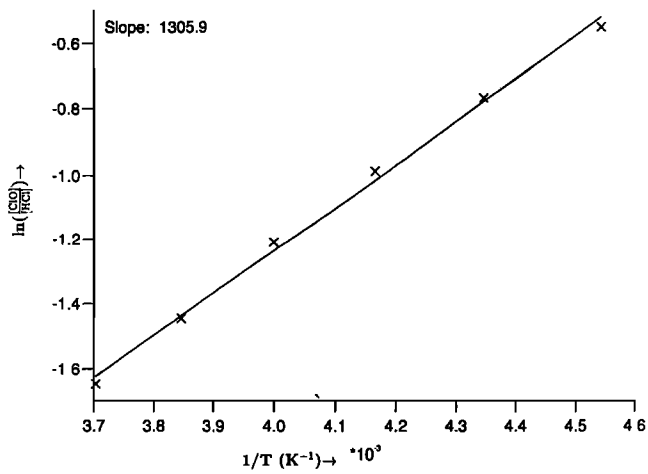

Figure 7. Temperature dependence of [ClO]/[HCl] at 1.5 hPa and at 58°N calculated from the photochemical box model.

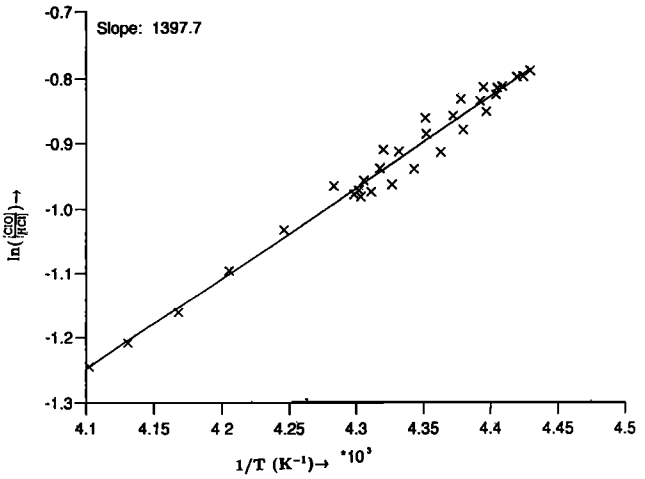

Figure 8. Temperature dependence of [ClO]/[HCl] at 1.5 hPa and at 58°N calculated from the EUGCM.

7.1. Error Analysis in the Photochemical Box Model

The main uncertainties in the photochemical box model are due to the uncertainties in laboratory measurements of rate constants. For second-order rate constants listed by *De More et al.* [1994], an estimate of the uncertainty at any given temperature is usually obtained from the following expression:

$$f(T) = f(298)\exp\left|\frac{\Delta E}{R}\left(\frac{1}{T} - \frac{1}{298}\right)\right| \qquad (8)$$

An upper or lower bound (corresponding approximately to 1 standard deviation) of the rate constant at any temperature T is obtained by multiplying or dividing the value of the rate constant at that temperature by the factor f(T). The quantities f(298) and $\Delta E/R$ the uncertainty in the rate constant at 298 K and in the Arrhenius temperature coefficient, respectively.

The uncertainty estimates for all the important second-order rate constants linked to ClOx chemistry are given in Table 1. The relevant procedures for estimating these uncertainties are outlined by *De More et al.* [1994]. Un-

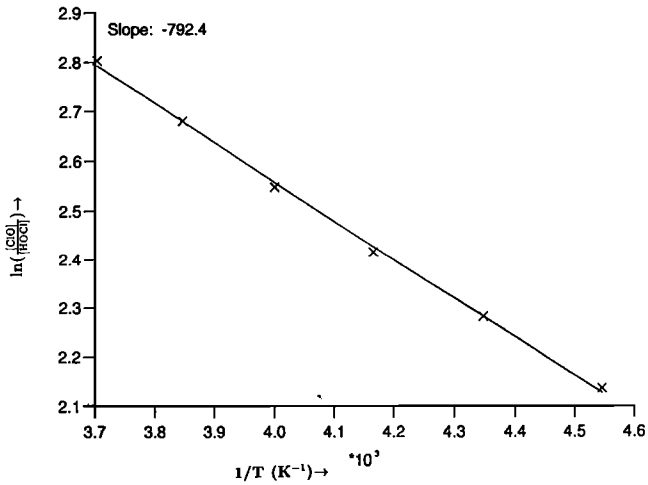

Figure 9. Temperature dependence of [ClO]/[HOCl] at 1.5 hPa and at 58°N calculated from the photochemical box model.

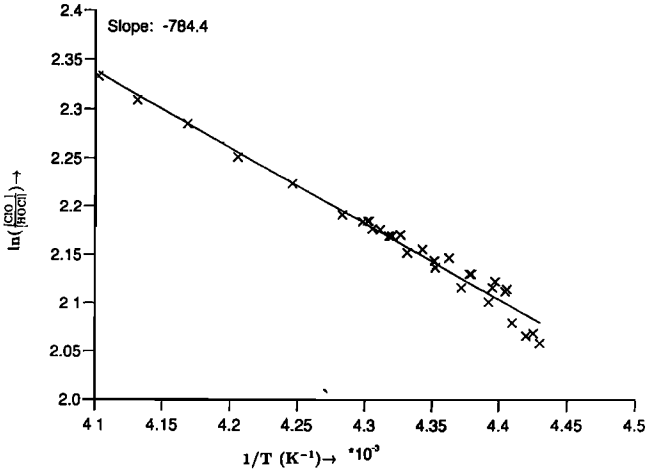

Figure 10. Temperature dependence of [ClO]/[HOCl] at 1.5 hPa and at 58°N calculated from the EUGCM.

certainty estimates associated with third body reactions (e.g., $ClO + NO_2 + M \rightarrow ClONO_2 + M$) are calculated by a different procedure also outlined by *De More et al.* [1994].

In this section, we focus our attention to two important reactions:

$$Cl + CH_4 \rightarrow CH_3 + HCl \qquad (k_5) \qquad (9)$$

a reaction which has a large temperature dependence and where $\pm\Delta E/R$ is about 10% of $\pm$E/R, and

$$Cl + O_3 \rightarrow ClO + O_2 \qquad (k_2) \qquad (10)$$

which has a moderate temperature dependence, but the uncertainty $\pm\Delta E/R$ is comparable to the magnitude of $\pm$ E/R (see Table 1).

After estimating the upper and lower bounds for the uncertainties associated with k_5 and k_2, we examined what effect these would have in the actual temperature dependence of [ClO], [ClO]/[HOCl], and [ClO]/[HCl]. The results are tabulated in Table 4.

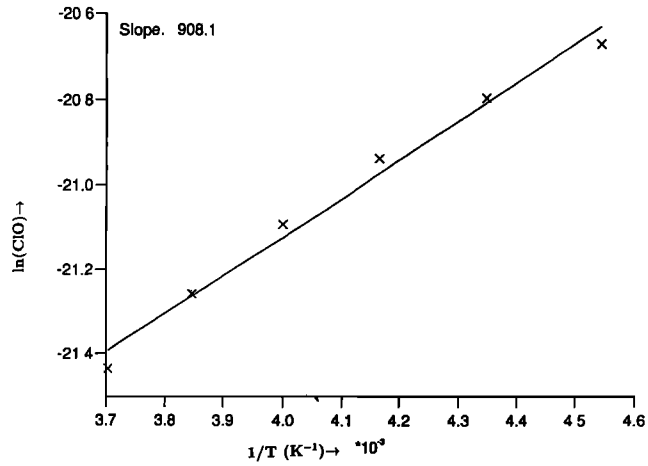

Figure 11. Temperature dependence of ClO at 1.5 hPa and at 58°N from the photochemical Box Model with varying solar zenith angles.

Table 4. Temperature Dependence With Uncertainties in Rate Constants

Uncertainty Description	Temperature Dependence, K		
	[ClO]	[ClO]/[HOCl]	[ClO]/[HCl]
k_2 (lower bound)	915.6	-812.2	1249.4
k_2 (upper bound)	907.2	-748.7	1384.3
k_5 (lower bound)	903.6	-745.0	1332.9
k_5 (upper bound)	896.6	-823.8	1247.0
No uncertainty	908.2	-792.5	1306.0

We first examine the sensitivity to k_5 (reaction (9)). If k_5 is increased (upper bound case), then the temperature dependence of [ClO] decreases, while the temperature dependence of [ClO]/[HOCl] increases. If, however, k_5 is decreased (lower bound case), then it is expected that less chlorine is converted and more stays as ClO. The overall effect on the ClO temperature dependence is that it decreases. It is important to emphasize that since ClOx chemistry is essentially nonlinear, changes to a particular rate constant initiate changes in a cycle of related reactions. In this section we focus our attention on how the temperature dependence changes as result of changes in the rate constants. In general, we find that uncertainties in k_2 (via equation (10)) evoke less substantial changes in the ClO temperature dependence as compared to what one would expect from the uncertainties in k_5.

However, from Table 4, we find that changes in the temperature dependence of [ClO], [ClO]/[HOCl], and [ClO]/[HCl] that result from changes in the magnitudes of k_2 and k_5 are always less than 5% and are significantly lower than the uncertainties encountered in the estimates of MLS ClO measurements.

7.2. Sensitivity to Selected Terms

An estimate of the individual contributions to the overall temperature dependencies in stratospheric chlorine chemistry could be obtained by differentiating equations (4) to (7) with respect to temperature, remembering that temperature dependence can arise from both the rate constants (e.g., k_5) and the species concentrations (e.g., $[O_3]$). Such an analysis would show that the contribution of a particular term depends on its own temperature dependence, weighted by its importance to chlorine chemistry. Here we highlight three terms which appear in equations (4) to (7) and which are important either because of their strong temperature dependencies or their importance in chlorine chemistry. The three terms considered are the two rate constants k_2 and k_5 and the ozone concentration, which has a temperature dependence of around 1000 K at the stratopause [*Barnett et al.*, 1975]. We have performed three further box model calculations in which the temperature dependence of these three terms are set to zero in order to determine their contribution to the ClO temperature dependence.

The rate constant k_2 is only weakly temperature dependent but is obviously a very important reaction in

stratospheric chlorine chemistry. Setting its temperature dependence to zero (by using the rate constant at 250 K, representing an average stratospheric temperature) has only a modest impact on the ClO temperature dependence, which rises to about 1030 K.

The two other terms, k_5 and ozone concentration, have much larger impacts. If the temperature dependence of k_5 is set to zero, the overall ClO temperature dependence is reduced to 200 K, a very weak dependence on temperature. If the temperature dependence of the ozone concentration is set to zero, the ClO temperature dependence falls to 680 K. It is clear that the overall temperature dependence calculated in the model depends on these two parameters and that the reaction between Cl and CH_4 is particularly important in determining the overall value. The overall temperature dependence depends on a balance of terms. The generally good agreement between model and observations suggests that the model has achieved the correct balance and does not indicate that there are major uncertainties in these aspects of stratospheric chlorine chemistry.

8. Conclusions

From an analysis of MLS ClO data near the stratopause where it is reasonable to assume that ClO is in photochemical equilibrium, we find a strong temperature dependence of the order of 1000 K(±200 K) including the effects of scaling and the bias uncertainties in the retrieved MLS data. Results from a three- dimensional model (EUGCM) agree well with the MLS results; we obtain a temperature dependence of 950 K in the three-dimensional model. The temperature dependencies obtained from the MLS data and the EUGCM agree quite well with results from a purely photochemical box model which yields a temperature dependence of the order of 900 K. Analysis of selected components in the chemical scheme of the box model suggests that the overall temperature dependence of ClO depends strongly on both the temperature dependence of the reaction between Cl and CH_4 and on the temperature dependence of the ozone concentration. The generally good agreement between the temperature dependence of ClO obtained from the MLS measurements, from both the photochemical model and the three-dimensional general circulation model does not suggest that there are major uncertainties in our understanding of the ClO chemistry in the upper stratosphere.

References

Barnett, J. J., J. T. Houghton, and J.A. Pyle, The temperature dependence of the ozone concentration near the stratopause, *Q. J. R. Meteorol. Soc., 101,* 245-257, 1975.

Brasseur, G., and S. Solomon, *Aeronomy of the middle atmosphere*, D. Reidel, Norwell, Mass., 1986.

Chipperfield, M. P., and J. A. Pyle, two-Dimensional modeling of northern hemisphere high-latitude lower stratosphere, *J. Geophys. Res., 95,* 11865-11874, 1990.

De More, W. B., D. M.Golden, R. F.Hampson, M. J.Kurylo, C. J. Howard, A. R. Ravishankara, C. E. Kolb, and M. J. Molina, Chemical kinetics and photochemical data for use in stratospheric modeling, *JPL Publ., 92-20,* 1994.

Dessler, A. E., S. R. Kawa, A. R. Douglass, D. B. Considine, J. B. Kumer, A. E. Roche, J. L. Mergenthaler, J. W. Waters, J. M. Russell III, and J. C. Gille, A test of the partitioning between ClO and $ClONO_2$ using simultaneous UARS measurements of ClO, NO_2, and $ClONO_2$, *J. Geophys. Res., 101,* 12515-12521, 1996.

Farman, J. C., B. G. Gardiner, and J. D. Shanklin, Large losses of total ozone in Antarctica reveal seasonal ClOx/NOx interaction, *Nature, 315,* 207-210, 1985.

Fishbein, E. F. et al., Validation of UARS Microwave Limb Sounder temperature and pressure measurements, *J. Geophys. Res., 101,* 9983-10,016

Froidevaux, L., M. Allen, S. Berman, and A. Daughton, The mean ozone profile and its temperature sensitivity in the upper stratosphere and lower mesosphere, *J. Geophys. Res., 94,* 6389-6417, 1989.

Froidevaux, L., J. Waters, W. G. Read, L. S. Elson, D. A. Flower, and R.F. Jarnot, Global ozone observations from the UARS MLS: An overview of zonal- mean results, *J. Atmos. Sci., 51,* 2846-2860, 1994.

Gray, L., M. Blackburn, M. P. Chipperfield, J. D. Haigh, D. Jackson, K. P. Shine, J. Thuburn, and W. Zhong First results from a 3-dimensional middle atmosphere model, *Adv. Space Res., 13,* (1), 363-372, 1993.

Haigh, J. D., Radiative heating in the lower stratosphere and the distribution of ozone in a 2-dimensional model, *Q. J. R. Meteorol. Soc., 110,* 167-185, 1984.

Lary, D. J., J. A. Pyle, and G. Carver, A 3-dimensional model study of nitrogen-oxides in the stratosphere, *J. Geophys. Res., 120,* 453-482, 1994.

Mahlman, J. D., and L. J. Umscheid, Comprehensive modeling of the middle atmosphere: the influence of horizontal resolution, in *Transport Processes in the Middle Atmosphere*, edited by G. Visconti and R. Garcia, pp. 251-266, D. Reidel, Norwell, Mass., 1987.

Manney, G.L., et al., Chemical depletion of ozone in the Arctic lower stratosphere during winter 1992-93, *Nature, 370,* 429-434, 1994.

Molina, M. J., and F. S. Rowland, Stratospheric sink for chlorofluoromethanes: chlorine-atom catalysed destruction of ozone, *Nature, 249,* 810-814, 1974.

Morcrette, J.J., Impact of changes to the radiation transfer parameterisation plus cloud optical properties in the ECMWF Model, *Mon. Weather Rev., 118,* 847-873, 1990.

Palmer, T. N., G. J. Shutts, and R. Swinbank, Alleviation of a systematic westerly bias in general circulation and numerical weather prediction models through an orographic gravity wave drag parameterization, *Q. J. R. Meteorol. Soc., 112,* 1001-1039, 1986.

Rind, D., R. Suozzo, N. K. Balachandran, A. Lacis, and G. Russell, The GISS global climate-middle atmosphere model, I, Model structure and climatology, *J. Atmos. Sci., 45,* 329-370, 1988.

Waters, J. W., L. Froidevaux, W. G. Read, G. L. Manney, L. S. Elson, D. A. Fowler, R. F. Jarnot, and R. S. Harwood, Stratospheric ClO and ozone from the Microwwave Limb Sounder on the Upper Atmosphere Research Satellite, *Nature, 362,* 597-607, 1993.

Waters, J. W., et al., Validation of UARS MLS ClO Measurements, *J. Geophys. Res., 101,* 10,091-10,127, 1996.

World Meteorological Organization (WMO), Scientific assessment of Ozone Depletion, Global Ozone Res. and Monit. Proj. *Rep. 37,* Washington, D. C., 1994.

S. Ghosh, Department of Physics, University of Manchester Institute of Science and Technology, Manchester M60 1QD, England.

P. Good and J. A. Pyle, Center for Atmospheric Science Department of Chemistry, Cambridge University, Cambridge CB2 1EW, England.

(Received June 13, 1995; revised January 24, 1997; accepted March 13, 1997.)